Modeling of light scattering in different regimes of surface roughness

Sven Schröder,[1,*] Angela Duparré,[1] Luisa Coriand,[1,2] Andreas Tünnermann,[1,2] Dayana H. Penalver,[3] and James E. Harvey[3]

[1]*Fraunhofer Institute for Applied Optics and Precision Engineering, Albert-Einstein-Straße 7, 07745 Jena, Germany*
[2]*Friedrich-Schiller-University, Institute of Applied Physics, Max-Wien-Platz 1, 07743 Jena, Germany*
[3]*University of Central Florida, College of Optics and Photonics / CREOL, 4000 Central Florida Boulevard, Orlando, Florida 32816-2700, USA*
**sven.schroeder@iof.fraunhofer.de*

Abstract: The light scattering of rough metallic surfaces with roughness levels ranging from a few to several hundred nanometers is modeled and compared to experimental data. Different modeling approaches such as the classical Rayleigh-Rice vector perturbation theory and the new Generalized Harvey-Shack theory are used and critically assessed with respect to ranges of validity, accuracy, and practicability. Based on theoretical calculations and comparisons with Rigorous Coupled Wave Analysis for sinusoidal phase gratings, it is demonstrated that the approximate scatter models yield surprisingly accurate results and at the same time provide insight into light scattering phenomena. For stochastically rough metal surfaces, the predicted angles resolved scattering is compared to experimental results at 325 nm, 532 nm, and 1064 nm. In addition, the possibilities of retrieving roughness information from measured scattering data for different roughness regimes are discussed.

OCIS codes: (290.0290) Scattering; (290.5835) Scattering, Harvey; (240.5770) Optics at surfaces, roughness, (120.6660) Surfaces measurements, roughness.

References and links

1. E. L. Church and P. Z. Takacs, "Specification of surface figure and finish in terms of system performance," Appl. Opt. **32**(19), 3344–3353 (1993).
2. J. E. Harvey, K. L. Lewotsky, and A. Kotha, "Effects of surface scatter on the optical performance of x-ray synchrotron beam-line mirrors," Appl. Opt. **34**(16), 3024–3032 (1995).
3. A. Duparré, "Scattering from surfaces and thin films," in *Encyclopedia of Modern Optics*, B. D. Guenther, D. G. Steel, and L. Bayvel, eds. (Elsevier, 2004).
4. C. Rockstuhl, S. Fahr, K. Bittkau, T. Beckers, R. Carius, F.-J. Haug, T. Söderström, C. Ballif, and F. Lederer, "Comparison and optimization of randomly textured surfaces in thin-film solar cells," Opt. Express **18**(S3 Suppl 3), A335–A341 (2010).
5. S. Schröder, A. Duparré, K. Füchsel, N. Kaiser, A. Tünnermann, and J. E. Harvey, "Scattering of Roughened TCO Films - Modeling and Measurement," in Optical Interference Coatings, OSA Technical Digest (Optical Society of America, 2010), paper ThD3.
6. M. Flemming, L. Coriand, and A. Duparré, "Ultra-hydrophobicity through stochastic surface roughness," J. Adhes. Sci. Technol. **23**(3), 381–400 (2009).
7. S. Schröder, A. Duparré, "Finish assessment of complex surfaces by advanced light scattering techniques," Proc. SPIE 7102, paper 0F (2008).
8. T. M. Elfouhaily and C. A. Guerin, "A critical survey of approximate scattering wave theories from random rough surfaces," Waves Random Media **14**(4), R1–R40 (2004).
9. P. Beckmann and A. Spizzichino, *The Scattering of Electromagnetic Waves from Rough Surfaces*, (Pergamon Press, 1963).
10. S. O. Rice, "Reflection of electromagnetic waves from slightly rough surfaces," Commun. Pure Appl. Math. **4**(2-3), 351–378 (1951).
11. E. L. Church, H. A. Jenkinson, and J. M. Zavada, "Relationship #res," Opt. Eng. **18**, 125 (1979).
12. J. M. Elson and J. M. Bennett, "Vector scattering theory," Opt. Eng. **18**, 116–124 (1979).
13. J. C. Stover, *Optical Scattering, Measurement and Analysis*, 2nd ed. (SPIE Press, 1995).

#142704 - $15.00 USD Received 14 Feb 2011; revised 7 Apr 2011; accepted 1 May 2011; published 5 May 2011

14. J. E. Harvey, "Light-scattering characteristics of optical surfaces," Ph.D. Dissertation, University of Arizona (1976).
15. T. V. Vorburger, E. Marx, and T. R. Lettieri, "Regimes of surface roughness measurable with light scattering," Appl. Opt. **32**(19), 3401–3408 (1993).
16. J. E. Harvey, N. Choi, and A. Krywonos, "Scattering from moderately rough interfaces between two arbitrary media," Proc. SPIE **7794**, 77940V, 77940V-11 (2010).
17. M. G. Moharam and T. K. Gaylord, "Rigorous coupled-wave analysis of grating diffraction—E-mode polarization and losses," J. Opt. Soc. Am. **73**(4), 451–455 (1983).
18. A. Taflove and S. C. Hagness, *Computational Electrodynamics: The Finite-Difference Time-Domain Method*, 2nd ed. (Artech House, 2000).
19. E. L. Church, "Statistical effects in the measurement and characterization of smooth scattering surfaces," Proc. SPIE **511**, 18 (1984).
20. A. Duparré, J. Ferre-Borrull, S. Gliech, G. Notni, J. Steinert, and J. M. Bennett, "Surface characterization techniques for determining the root-mean-square roughness and power spectral densities of optical components," Appl. Opt. **41**(1), 154–171 (2002).
21. "Optics and optical instruments-test methods for radiation scattered by optical components," ISO 13696:2002 (International Organization for Standardization, 2002).
22. J. E. Harvey, A. Krywonos, and C. L. Vernold, "Modified Beckmann-Kirchhoff scattering model for rough surfaces with large incident and scattering angles," Opt. Eng. **46**(7), 078002 (2007).
23. M. Trost, S. Schröder, T. Feigl, A. Duparré, and A. Tünnermann, "Influence of the substrate finish and thin film roughness on the optical performance of Mo/Si multilayers," Appl. Opt. **50**(9), C148–C153 (2011).
24. A. Krywonos, "Predicting surface scatter using a linear systems formulation of non-paraxial scalar diffraction," Ph.D. Dissertation, College of Optics and Photonics, University of Central Florida (2006).
25. J. E. Harvey, N. Choi, A. Krywonos, and J. Marcen, "Calculating BRDFs from surface PSDs for moderately rough surfaces," Proc. SPIE **7426**, 74260I, 74260I-9 (2009).
26. A. Krywonos, J. E. Harvey, and N. Choi, "Linear systems formulation of scattering theory for rough surfaces with arbitrary incident and scattering angles," Accepted for publication in J. Opt. Soc. Am. A (March 25, 2011)
27. J. C. Stover, "Experimental confirmation of the Rayleigh-Rice obliquity factor," Proc. SPIE **7792**, 77920J, 77920J-5 (2010).
28. S. Schröder, T. Herffurth, H. Blaschke, and A. Duparré, "Angle-resolved scattering: an effective method for characterizing thin-film coatings," Appl. Opt. **50**(9), C164–C171 (2011).
29. A. von Finck, M. Hauptvogel, and A. Duparré, "Instrument for close-to-process light scatter measurements of thin film coatings and substrates," in Optical Interference Coatings, OSA Technical Digest (Optical Society of America, 2010), paper ThD4.
30. J. E. Harvey, A. Krywonos, and D. Bogunovic, "Nonparaxial scalar treatment of sinusoidal phase gratings," J. Opt. Soc. Am. A **23**(4), 858–865 (2006).

1. Introduction

The scattering properties of optical and non-optical surfaces are strongly related to the surface structure with respect to the incident wavelength. For optical imaging surfaces light scattering is usually an unwanted effect caused by surface imperfections and fabrication errors [1–3]. Although several optical applications make use of rough interfaces to tailor the light distribution, such as optical diffusors or structured thin film solar cells [4,5]. For many of these applications predicting the light scattering properties from surface roughness metrology data is desirable.

Also for non-optical, technical surfaces, surface roughness can play a crucial role for the functional properties, such as wetting, mechanical stability, conductivity and others [6]. Light scattering measurement and analysis is a powerful way to determine roughness properties in a fast, robust, non-contact, and yet sensitive way [7]. For this purpose, models are required that allow for solving the inverse scattering problem in order to retrieve roughness information from light scattering measurement data.

Approaches for modeling the light scattering from rough surfaces may be divided in analytic scattering models and rigorous treatments.

Analytic scattering theories are based on Maxwell's equations but make use of certain approximations to solve them, which results in different limitations of their ranges of validity [8]. Yet, analytic models have several advantages: They are usually rather easy to calculate, they provide direct insight into the scattering process, and they often provide an inverse solution of scattering problem. The most prominent analytical scattering theories are the classical Beckmann-Kirchhoff theory [9], the Rayleigh-Rice or Vector Perturbation theory

#142704 - $15.00 USD Received 14 Feb 2011; revised 7 Apr 2011; accepted 1 May 2011; published 5 May 2011

[10–13], and the classical Harvey-Shack scattering theory [14], each having their specific advantages and limitations [15]. In addition, a new Generalized Harvey-Shack theory has been developed recently that combines the advantages of existing analytical models without having their limitations [16]. All of the aforementioned analytical approaches make use of the statistical properties of stochastic surfaces instead of relying on the knowledge of the exact topography. This has the advantage of inherent ensemble averaging.

Rigorous electromagnetic theories offer exact solutions to the scattering problem. Different approaches exist such as the Rigorous Coupled Wave Analysis (RCWA) [17] and the Finite Difference Time Domain (FDTD) method [18], with different advantages and capabilities regarding the handling different surface structures. They are most powerful in calculating the scattering of one dimensional periodic surfaces. Any additional degree of complexity usually requires a tremendously increased computational power, approximations at the cost of accuracy, or is not possible at all. Furthermore, statistical effects of surface scattering that are extensively discussed in papers about analytical models [19] are often neglected in rigorous treatments. Finally, none of the rigorous approaches allows for solving the inverse problem of obtaining roughness information from surface light scattering data directly. Nevertheless, rigorous treatments for the first time enabled the calculation of light scattering properties also for surface structures beyond the ranges of validity of existing analytic models. They can therefore be extremely useful in order to assess the accuracy of different analytic approaches.

A stochastically rough surface structure can be seen as a superposition of a large number of sinusoidal phase gratings with different orientations, periods, amplitudes, and phases. Hence, we start our investigation with diffraction efficiency calculations for simple sinusoidal phase gratings as special types of rough surfaces using different theoretical models. We then analyze the angle resolved scattering of stochastically rough metal surfaces by comparing the predictions of different scattering theories with experimental results at different wavelengths.

This paper is organized as follows. In Sec. 2 the fundamental quantities to describe surface roughness and light scattering are summarized. A brief summary of surface scattering theories is given in Sec. 3. The experimental set-ups and procedures used are presented in Sec. 4. In Sec. 5 modeling results of the diffraction efficiency of sinusoidal phase gratings are discussed. In Sec. 6 light scattering measurement and modeling results for rough metallic surfaces are presented and discussed.

2. Definitions

2.1 Surface roughness

In the following we will give a brief summary of the statistical description of roughness. More detailed information can be found in [1,13,20].

The 2-dimensional Power Spectral Density function PSD is defined as the squared modulus of the Fourier transform of the interface topography:

$$PSD_2(f_x, f_y) = \lim_{L\to\infty} \frac{1}{L^2} \left| \int_0^L \int_0^L z(x,y)\, e^{-2\pi i(f_x x + f_y y)} \mathrm{d}x\mathrm{d}y \right|^2 . \qquad (1)$$

Hereby we have assumed that the surface topography $z(x,y)$ has zero mean. L is the length of the scanned profile.

The PSD expresses the power of different roughness components in terms of the (lateral) surface spatial frequencies f_x and f_y. It contains all statistical information of random-rough (stochastic) surfaces such as generated by grinding, polishing, etching, as well as thin film growth or erosion.

#142704 - $15.00 USD Received 14 Feb 2011; revised 7 Apr 2011; accepted 1 May 2011; published 5 May 2011

Stochastic surfaces often exhibit isotropic roughness corresponding to a PSD with a polar symmetry. The 2D-isotropic PSD is calculated by averaging the 2D PSD over all azimuthal directions:

$$PSD(f) = \frac{1}{2\pi}\int_0^{2\pi} PSD(f,\psi)\mathrm{d}\psi \,. \tag{2}$$

Using the transformations $f = \sqrt{f_x^2 + f_y^2}$ and $\psi = \arctan(f_y / f_x)$.

Every real profile or roughness measurement technique is confined to a certain spatial frequency range, which is limited, for instance, by the investigated surface area and the instrumental resolution. The (bandwidth limited) rms roughness, usually defined as the square root of the standard deviation of $z(x,y)$ from its mean value can be calculated by integrating the PSD:

$$\sigma = \left[2\pi \int_{f_{\min}}^{f_{\max}} PSD(f)\, f\, \mathrm{d}f \right]^{\frac{1}{2}} . \tag{3}$$

The integration limits depend on the application at hand or measurement technique used. In the extreme case $f_{\min} = 0$ and $f_{\min} = \infty$, σ is called the total roughness.

Another description of surface roughness is provided by the surface autocovariance function ACV. The correlation length τ_c is defined as the lateral spacing at which the ACV drops to 1/e of its maximum value. The ACV and PSD contain both vertical and lateral information about surface roughness (e.g. rms roughness and correlation length). They form a Fourier transform pair and are thus equivalent. However, only PSDs provide a direct representation of bandwidth limits. Moreover, using PSDs we are able to combine roughness information from different roughness measurement techniques to retrieve multi scale roughness information.

In practice, surface topography is sampled with a finite number of points. The integral expressions given above are therefore replaced by discrete forms [13], sometimes introducing apodization functions to suppress numerical artifacts.

2.2 Light scattering

The following summary is based on the assumption of isotropic surface roughness, which is usually justified for ground, polished, and coated surfaces. For normal incidence, the scattering is therefore a function of the polar angle θ_s only.

Angle Resolved Scattering (ARS) is defined as the power ΔP_s scattered into a small solid angle $\Delta\Omega_s$ normalized to that solid angle and the incident power P_i:

$$ARS(\theta_s) = \frac{\Delta P_s(\theta_s)}{\Delta\Omega_s P_i} \,. \tag{4}$$

ARS is related to the Bidirectional Scattering Distribution Function (BSDF) by: $BSDF(\theta_s) = ARS(\theta_s) / \cos(\theta_s)$. It should also be noted that the correct radiometric expression for ARS would be normalized scattered intensity. However, various definitions of intensity are used in different communities. In order to emphasize the essential normalizations according to Eq. (4), we use the term ARS.

Several definitions of quantities exist that define integrated scattering such as the Total Integrated Scatter (TIS), Haze, and Total Scattering (TS), the latter being defined in the international standard ISO 13696 [21]. Total backscattering (TS_b) is defined as the power P_s scattered from a surface into the backward hemisphere normalized to the incident power P_i.

#142704 - $15.00 USD Received 14 Feb 2011; revised 7 Apr 2011; accepted 1 May 2011; published 5 May 2011

For normal incidence, the standard requires at least the light scattered within the angular range between 2° and 85° to be collected. From Eq. (4) it follows that:

$$TS_b = \frac{P_s}{P_i} = 2\pi \int_{2^\circ}^{85^\circ} ARS(\theta_s) \sin\theta_s \mathrm{d}\theta_s \ . \tag{5}$$

The starting point of scattering theories that link the surface structural properties and the light scattering properties are always Maxwell's equations. However certain approximations are used to find a solution to the rather complex problem of scattering from certain structures.

3. Surface scattering models

3.1 Beckmann-Kirchhoff (BK) theory

The famous Beckmann-Kirchhoff theory [9] is a scalar treatment. Based on the Kirchhoff diffraction integral, Beckmann derived an expression for the "scattering efficiency" in form of an infinite sum. Closed form solutions only exist for very smooth surfaces ($\sigma / \lambda << 1$) and very rough surfaces ($\sigma / \lambda >> 1$) with Gaussian ACVs. In addition, it has been pointed out that the classical BK theory contains an implicit paraxial limitation [22].

3.2 Rayleigh-Rice (RR) theory

The Rayleigh-Rice vector perturbation approach can be seen as the most rigorous analytical solution of Maxwell's equations for the limiting case of vanishing surface roughness (smooth surface limit) [10–13]. The result is a direct and rather simple relationship between the ARS and the surface PSD:

$$ARS(\theta_s) = \frac{16\pi^2}{\lambda^4} \gamma_i \gamma_s^2 \theta_s \, Q \, \mathrm{PSD}(f) \, . \tag{6}$$

Hereby, $\gamma_i = \cos\theta_i$ and $\gamma_s = \cos\theta_s$ are the cosines of the incident and the scattering angles, respectively. Q is the angle dependent polarization reflectance, an optical factor that contains information about the dielectric function as well as about the conditions of illumination and detection (angles of incidence and scattering, polarization, etc.).

The link between spatial frequencies and scattering angles is given by the grating equation: $f = \left|\sin\theta_s - \sin\theta_i\right| / \lambda$. Hence, in the smooth surface regime, the ARS merely consists of the first diffraction orders of the surface spectral components.

The rather simple and direct relationship between the ARS and the surface PSD provided by the Rayleigh-Rice result is of crucial importance for the characterization of surface roughness using light scattering techniques [7,13,23]. However, the smooth surface requirement can be a severe restriction depending on the surface or wavelength at hand. It is usually formulated as: $\sigma / \lambda << 1$, although a more accurate criterion is [13]: $(4\pi\sigma_{rel} \cos\theta_i / \lambda)^2 << 1$. Unfortunately, there is no distinct number to decide whether the criterion is fulfilled or not. In [13] it is stated that σ / λ should be smaller than 0.01. In [15] it was concluded that σ / λ should be smaller than 0.05. In particular at short wavelengths the smooth surface requirement is likely to be violated. Yet this does not necessarily mean that the RR theory fails completely as will be demonstrated in this paper.

3.3 Generalized Harvey-Shack (GHS) theory

Recently, a new theory has been developed by Krywonos and Harvey that is a generalization of the Fourier optics treatment of light scattering known as the Harvey-Shack theory. Based on the Helmholtz equation it is basically a scalar theory. The scattering behavior of a rough

#142704 - $15.00 USD Received 14 Feb 2011; revised 7 Apr 2011; accepted 1 May 2011; published 5 May 2011

surface with Gaussian height distribution function (but arbitrary PSD) is described using a surface transfer function [24–26]:

$$H_s(\hat{x},\hat{y};\gamma_i,\gamma_s) = \exp\left\{-\left[2\pi\hat{\sigma}_{rel}(\gamma_i+\gamma_s)\right]^2\left[1-\frac{ACV(\hat{x},\hat{y})}{\sigma_{total}^2}\right]\right\}, \tag{7}$$

where $\hat{x} = x/\lambda$ and $\hat{y} = y/\lambda$ are the normalized coordinates, $\hat{\sigma}_{rel} = \sigma_{rel}/\lambda$ is the normalized rms roughness relevant for diffuse scattering. For normal incidence this relevant roughness corresponds to the square root of the integral of the PSD from $f = 0$ to $1/\lambda$ [Eq. (3)].

The ARS is merely the Fourier transform of the GHS surface transfer function multiplied with the total reflectance of the surface and the cosine of the scattering angle according to Lambert's law. The total reflectance might be replaced by the optical factor Q from the Rayleigh-Rice result to take into account polarization properties. Harvey refers to this procedure as "borrowing" the Rayleigh-Rice optical factor. For small incident and scatter angles it can be shown that Q is equal to the total reflectance [13]. This intuitive quasi-vectorization therefore provides results that are at least as accurate as the purely scalar approach in general. The final GHS result therefore becomes:

$$ARS(\theta_s) = Q\gamma_s \mathsf{F}\left\{H_s(\hat{x},\hat{y};\gamma_i,\gamma_s)\right\} \ . \tag{8}$$

For smooth surfaces the exponential function in the surface transfer function [Eq. (7)] can be approximated and Eq. (9) transforms into the Rayleigh-Rice result except for a slightly different obliquity factor [27].

The GHS modeling procedure for a given surface is as follows [25]: (i) measurement of the surface PSD over the entire range of relevant spatial frequencies, usually through combining different techniques, (ii) fit of a combination of ABC-model PSDs [1] to the experimental data, (iii) analytical calculation of the ACV, (iv) determination of the surface transfer functions for the given incident angle and any scatter angle, and (v) calculation of the ARS according to Eq. (8) using a Fourier transformation in log-space.

Although more computationally intensive, the new GHS theory seems to combine the advantages of the Rayleigh-Rice and the Beckmann-Kirchhoff theories with the limitations of neither. The only theoretical limitations are that it is still a scalar approach in nature (even though the final result has been quasi-vectorized) and it does not account for higher order effects such as multiple scattering. Not surprisingly, solving the inverse scattering problem, hence retrieving roughness information from light scatter data, is not possible in general using the GHS theory. In this paper we are going to investigate and critically evaluate the validity and capabilities of the new approach.

3.4 Rigorous treatments

Rigorous treatments are with some justification usually seen as providing exact solutions to the scattering problem without any approximations. However, in practical applications involving three-dimensional stochastic surfaces, the large number of parameters requires a tremendous amount of computational power and time that finally demand approximations in the input data. For example, a typical surface profile measured using atomic force microscopy has 512x512 data points. The investigated surface area has to be small enough to resolve all structural features that are (supposedly) relevant for the scattering properties. On the other hand, a considerable number of relevant features have to be included in order to achieve a sufficiently large averaging of the scattering characteristics of the individual features. It is therefore obvious that even rigorous treatments are finally confronted with approximations be it on the calculation side or on the data input side.

Several rigorous treatments have been developed during the last few decades, where certain approaches are more suited for specific problems than others. Typical criteria that lead

#142704 - $15.00 USD Received 14 Feb 2011; revised 7 Apr 2011; accepted 1 May 2011; published 5 May 2011

to the decision for one or another approach are deterministic or stochastic surfaces, single surfaces or multilayer structures, size of relevant surface features with respect to the wavelength of light, as well as considerations with respect to complexity, accuracy, efficiency, and speed.

For calculations of the diffraction efficiency of periodic grating structures, the Rigorous Coupled Wave Analysis (RCWA) developed by Moharam et. al [17] seems to be particularly powerful. The RCWA calculations in this paper were performed using an algorithm developed at CREOL as well as with the software MIST developed by Thomas Germer at NIST, Gaithersburg, USA. Both implementations were found to be in excellent agreement with each other.

The Finite Difference Time Domain (FDTD) method can be used to predict the scattering of stochastically rough surfaces based on measured surface topography data. Scatter predictions using the FDTD method have been presented recently [4] and are also under investigation for the surfaces discussed in the present paper. Yet, we believe that questions regarding how to appropriately take into account the influence of the topography at different lateral scales, which is of particular importance for statistically roughened surfaces, and the absolute normalization of the results require a detailed discussion that is beyond the scope of this paper. Instead, we focus on comparing the results of analytic theories and rigorous treatments for simple sinusoidal diffraction gratings. For this purpose the well established RCWA method can be used that provides rapid results and insight into the limits of validity of the different models.

4. Experimental

4.1 Sample generation

The preliminary investigations of sinusoidal phase gratings are purely based on computer calculations. Yet, in one case parameters similar to those of a real grating analyzed in [27] were used.

For the investigations of stochastically rough surfaces, raw disks with a diameter of 25 mm and a thickness of 5 mm were cut from a steel cylinder (stainless steel X5CrNi18-10) using a turning machine. As a result, all raw disks exhibited typical anisotropic ring structures. Different grinding and polishing procedures were then applied to remove the turning marks and to generate surface structures with a large variety of roughness levels ranging from optically smooth to rough.

4.2 Roughness measurements

Stochastic surfaces usually exhibit surface features over a wide range of spatial frequencies. For a thorough roughness analysis different instruments and resolutions have to be used to cover the entire range of spatial frequencies relevant for the light scattering process.

The smallest relevant spatial frequency range can be estimated using the fact that in the smooth surface regime, the RR theory predicts the ARS to merely consist of the first diffraction orders of the surface spectral components. Consequently, for normal incidence spatial frequencies between $f = 1/D$ and $f = 1/\lambda$ are directly relevant for the light scattering, where D denotes the diameter of the illuminated portion of the scattering surface. For typical applications, the low spatial frequency limit is in the order of $1/1000\ \mu m^{-1}$. The shortest wavelength employed for scatter measurements in this paper is 325 nm which corresponds to a high spatial frequency limit of $3\ \mu m^{-1}$. In order to sufficiently cover this large spatial frequency range, different roughness measurement techniques and measurement parameters were used.

White light interferometry (WLI) was performed using a Zygo NewView 600s with 2.5x and 50x objectives corresponding to fields of view of $2.8 \times 2.1\ mm^2$ and $141 \times 105\ \mu m^2$. While WLI is of great use to measure roughness components in the low- and mid-spatial frequency

#142704 - $15.00 USD Received 14 Feb 2011; revised 7 Apr 2011; accepted 1 May 2011; published 5 May 2011

range, the information at high spatial frequencies is always limited by the transfer function of the objective used.

Therefore, Atomic force microscopy (AFM) was performed to measure high spatial frequency roughness. An AFM VEECO D3100 operated in Tapping Mode with single crystalline Si probes (10 nm nominal tip radius) was used. Scan areas of 1x1 μm^2 and 10x10 μm^2, each scan containing 512x512 data points, were analyzed.

The output of each single AFM or WLI measurement is a 3D topography map containing roughness components in a certain spatial frequency range. From the single topographies, PSDs were calculated according to Eq. (6). All PSDs for a given surface were then combined to a single Master-PSD using the procedure described in detail in [20]. The combination of single measurements to a Master-PSD enables averaging of the roughness information in a certain spatial frequency range as well as substantially enhancing the total spatial frequency range. It is in particular for these both reasons that scatter calculations based on Master-PSDs are much more robust and representative for the given surface than calculations based on single scanned profiles, rigorous or not.

Knowledge of the real and imaginary parts of the index of refraction of the steel surfaces, n and k, are required to calculate the optical factor, Q, in Eqs. (6) and (8). For this purpose, specular reflectance measurements were performed on the smoothest surface (sample A). The spectral reflectance was measured using a commercial spectrometer Perkin Elmer Lambda 900. In addition, the reflectance as a function of the angle of incidence for both s- and p-polarized light at the wavelengths of interest were measured using the light scattering instrumentation described in the next section. Starting from the optical properties of iron, the optical constants were then adjusted to fit the measured reflectance data. The measured normal incidence reflectance R and optical constants at the wavelengths of interest are: (i) at 325 nm: $R = 48\%$, $n = 1.8$, $k = 2.5$, (ii) at 532 nm: $R = 59\%$, $n = 2.04$, $k = 3.3$, (iii) at 1064 nm: $R = 67\%$, $n = 2.06$, $k = 3.9$. Considering both the non-zero surface roughness and the uncertainty of the measurements, the relative uncertainty of the reflectance values is estimated to be below 3% at all wavelengths.

4.3 Light scattering measurements

Angle resolved light scattering measurements were performed at 325 nm, 532 nm, and 1064 nm. Using different wavelengths allows us to analyze a given sample at different roughness to wavelength ratios by using the same PSD. Since measuring a single ARS at a given wavelength is less cumbersome than determining a Master PSD by combining PSDs of numerous single topography measurements, this tremendously increases the accuracy and efficiency of our comparison. The wavelengths were chosen such that a surface that has to be considered to be rough at the shortest wavelength might still be optically smooth at the longest wavelength.

For the ARS measurements at 325 nm and 1064 nm, the instrument ALBATROSS (3D Arrangement for Laser Based Transmittance, Reflectance and Optical Scatter Measurement) developed at Fraunhofer IOF and presented in detail in [28] was used. A HeCd laser and a Nd:YAG laser were used for measurements at 325 nm and 1064 nm, respectively. A metallic mirror based spatial filter and several baffles are used for beam preparation and suppression of system stray light in order to minimize the instrument signature (scattering signal without sample present). The sample is located on a positioning system to adjust the irradiated position and the angle of incidence. The illumination spot diameter was adjusted to 3 mm. The detector, which is based on a side-on photomultiplier tube, can be rotated within the entire sphere around the sample. Yet, for the present investigation of merely isotropic surfaces, only in-plane measurements were performed. A detector aperture diameter of 2 mm was used corresponding to a detector solid angle $\Delta\Omega_s$ of $3x10^{-5}$ sr. The instrument exhibits a dynamic range of up to 15 orders of magnitude and a noise equivalent ARS level of down to 10^{-7} sr^{-1}.

#142704 - $15.00 USD Received 14 Feb 2011; revised 7 Apr 2011; accepted 1 May 2011; published 5 May 2011

In addition, for measurements at 532 nm a new table-top instrument was used that is described in detail in [29]. It exhibits similar features as the one described above in a much more compact design.

It should be noted that the choice of the diameters of both the illumination spot on the sample and the detector aperture for the light scattering measurements allows for sufficient ensemble averaging and suppression of surface speckle. In order to achieve a comparable amount of statistical stability of surface topography data, a large number of single measurements have to be combined. This is challenging but possible by combining the data to Master PSDs that can be used as input for the analytic models. For rigorous models, however, this means performing the entire calculations for numerous topographies at various sample positions with different resolutions and combining the final scattering curves. This requires a tremendous amount of computational power and time and the justification of this approach has to be put under careful investigation.

5. Diffraction efficiency of sinusoidal phase gratings

Before investigating real, stochastically rough metallic surfaces in detail, it might be useful to discuss the diffraction properties of simple sinusoidal phase gratings. Since a stochastically rough surface can be seen as a superposition of a sinusoidal phase gratings, this simple case can provide more insight into the scattering phenomenon and scatter models. We hereby follow a procedure that was presented recently by Stover to experimentally verify the RR theory [27].

The PSD of a sinusoidal grating with amplitude a is merely a delta function at a spatial frequency corresponding to the inverse period of the grating. It is straightforward to show that the Rayleigh-Rice result [Eq. (6)] leads to the following expression for the diffraction efficiency of the first order [13,27]:

$$P_1 / P_i = \left(\frac{2\pi a}{\lambda} \right)^2 Q \cos\theta_s \cos\theta_i \,. \tag{9}$$

The basis of the Harvey-Shack theory is the non-paraxial diffraction theory (NP) presented in [30]. For the sinusoidal grating, the efficiency for the m-th diffracted order is:

$$P_m / P_i = Q \frac{J_m^2\left(\frac{2\pi a}{\lambda} (\gamma_i + \gamma_s)^2 \right)}{\sum_{m=\min}^{\max} J_m^2\left(\frac{2\pi a}{\lambda} (\gamma_i + \gamma_s)^2 \right)} \,. \tag{10}$$

J_m is the Bessel function of the first kind, order m. The summation limits in the denominator of Eq. (4) are the minimum and maximum propagating order of diffraction. The sum therefore corresponds to a renormalization of the propagating orders when higher orders go evanescent. This renormalization to take into account the effect of evanescent orders is also a fundamental feature of the non-paraxial diffraction theory.

Following Stover's approach, for a given grating with period p and amplitude a, the angle of incidence was adjusted such that the first orders appear at (scatter) angles between 0 degrees and 90 degrees. The diffraction efficiencies were then calculated using the Rayleigh-Rice theory (RR) according to Eq. (9), the non-paraxial diffraction theory (NP) according to Eq. (10), as well as the Rigorous Coupled Wave Analysis (RCWA). The results for different grating parameters at a wavelength of 532 nm are shown in Fig. 1.

For the rather shallow grating with an amplitude of only 5 nm (Fig. 1(a)) the RR result is virtually identical with the RCWA result. This demonstrates that the RR theory can be considered to be exact for wavelength ratios $a/\lambda = 0.01$ and below. Also the NP prediction is

#142704 - $15.00 USD Received 14 Feb 2011; revised 7 Apr 2011; accepted 1 May 2011; published 5 May 2011

in good agreement with the RCWA result, although there is a slight disagreement at near grazing angles. This effect is a topic of ongoing discussion [27].

The results for a = 20 nm (Fig. 1(b)) indicate that for larger amplitudes, the RR theory starts to predict efficiencies too high at small angles. Yet the corresponding error is below 5% for $a/\lambda \leq 0.04$. This quantitative smooth-surface limit is in good agreement with former statements for stochastically rough surfaces [13,15] if the amplitude is seen as a measure for the rms roughness. The NP result remains accurate except for the deviation at large angles. The results for the same amplitude but larger period of p = 10 μm (Fig. 1(c)) reveal that this effect almost vanishes for larger periods corresponding to diffraction angles closer to the specular direction.

The cases for the substantially increased amplitude of 50 nm, 100 nm, and 300 nm (Fig. 1(d)–1(f)) illustrate that even far beyond the range where the RR theory is supposed to be valid, the NP theory yields results that are in excellent agreement with the RCWA result over almost the entire angular range. For the sake of completeness, the prediction of the classical Beckmann-Kirchhoff theory (BK) is also shown in Fig. 1(f), the results being substantially overestimated for diffraction angles greater than 30 degrees.

#142704 - $15.00 USD Received 14 Feb 2011; revised 7 Apr 2011; accepted 1 May 2011; published 5 May 2011

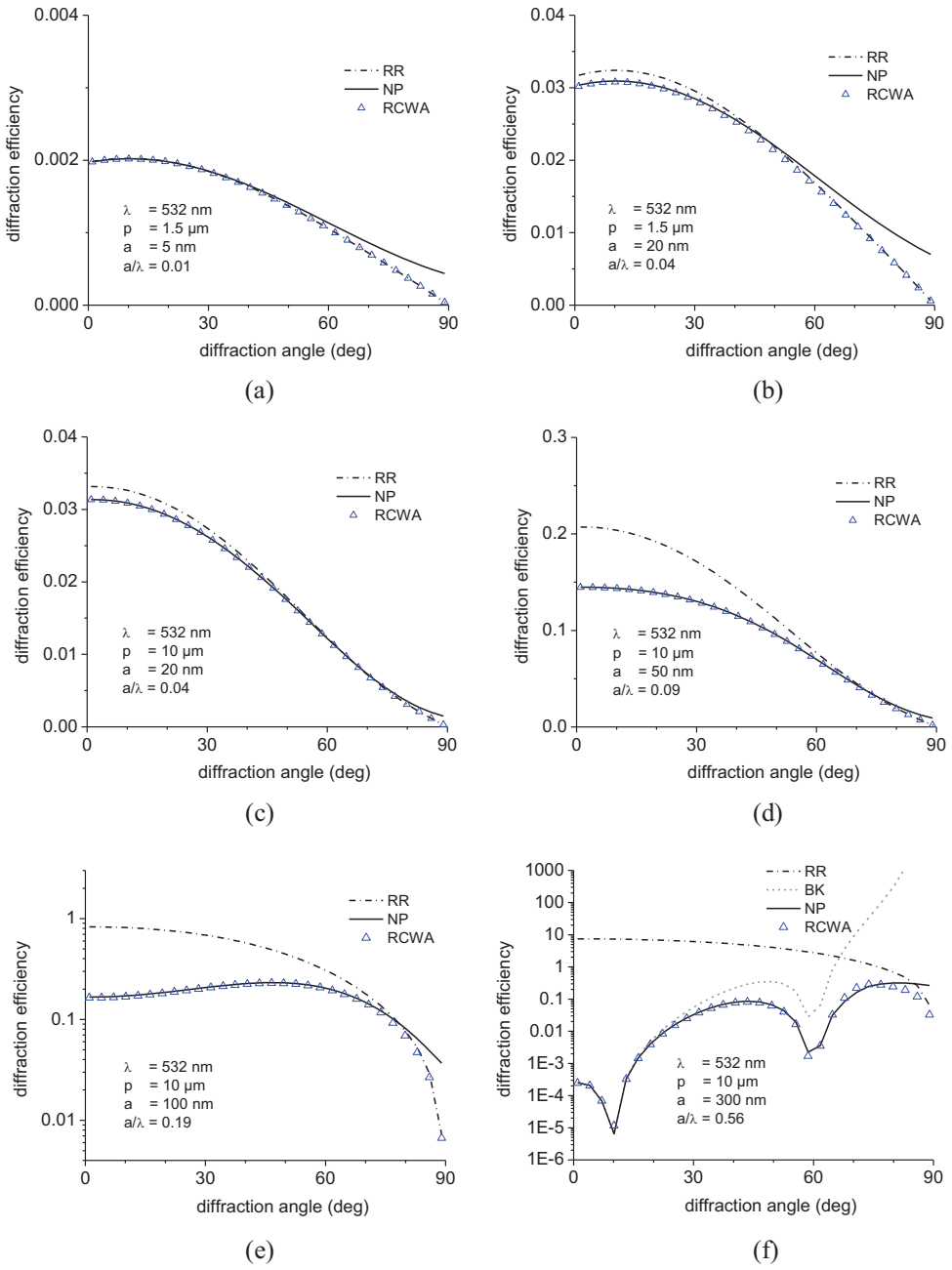

Fig. 1. First order scattering efficiency of sinusoidal phase gratings with different periods *p* and amplitudes *a* at a wavelength of 532 nm. Diffraction angles between 0 degrees and 90 degrees were achieved by adjusting the angle of incidence.

It is interesting to note that even in those cases that tremendously violate the smooth-surface criterion, the RR results are accurate at very large angles. It might therefore be possible to modify the NP result at large angles using the RR result. However, the good agreement of the NP and the RCWA results for all cases, and therefore the accuracy of the GHS theory, can be considered to be more than sufficient for the investigations in this paper.

#142704 - $15.00 USD Received 14 Feb 2011; revised 7 Apr 2011; accepted 1 May 2011; published 5 May 2011

Different parametrizations could have been used as well. However, the present approach allows to easily verify the presented results using a single-wavelength scatterometer.

6. Scattering of stochastically rough surfaces

The Power Spectral Density functions of the steel surfaces were measured using AFM and WLI as described in Sec. 4A. The Master-PSDs of all samples determined by combining the single PSDs are shown in Fig. 2.

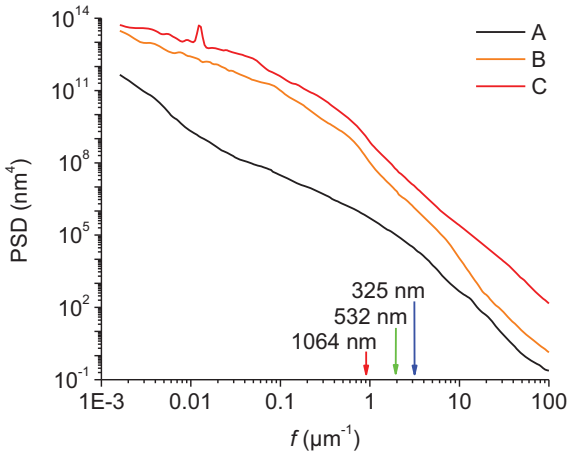

Fig. 2. Master-PSDs of steel surfaces. The arrows indicate the upper bandwidth limits of the relevant spatial frequency range for three illumination wavelengths and assuming normal incidence.

The PSDs reveal that a large variety of roughness spectra has been generated and combinations of ABC-model PSDs have to be used to fit the data. The peaks at 0.01 μm^{-1} in the PSD of samples C suggests that residual turning marks of the raw samples that have not been removed by the grinding process are present for this sample. Therefore, although care has been taken to generate isotropic roughness structures, the effects of anisotropic roughness might have to be taken into account when comparing light scattering measurements and predictions based on PSD data.

Band limited rms roughness values were calculated from the PSDs by numerical integration over the corresponding spatial frequency ranges. The total roughness corresponds to the square root of the total volume under the PSDs over the entire spatial frequency range. The relevant roughness for each wavelength was calculated using Eq. (3) with f_{min} = 1e-3 and $f_{max} = 1/\lambda$ for wavelengths of 325 nm, 532 nm and 1064 nm. The resulting upper bandwidth limits are indicated by arrows in Fig. 2.

The results for samples A, B, and C are summarized in Table 1. Although not listed explicitly it should be noted that the relevant roughness values are always close to but in no case identical with the total roughness, the maximum deviation being 8% for sample A at 1064 nm.

#142704 - $15.00 USD Received 14 Feb 2011; revised 7 Apr 2011; accepted 1 May 2011; published 5 May 2011

Table 1. Total rms Roughness and Ratio of Relevant Roughness to Wavelength for Samples A, B, and C

sample	σ_{total} (nm)	325 nm: σ_{rel} / λ	532 nm: σ_{rel} / λ	1064 nm: σ_{rel} / λ
A	6.0	0.018	0.011	0.005
B	135.7	0.41	0.25	0.12
C	322.2	0.98	0.50	0.30

With view to the results of Sec. 5 the roughness to wavelength ratios illustrate that sample A can be considered to be optically smooth at all three wavelengths, Sample C is very rough, and Sample B is an intermediate, moderately rough surface. Comparing the roughness to wavelength ratios of the stochastically rough surfaces and the sinusoidal phase gratings discussed in Sec. 5, it is interesting to note that at 1064 nm, samples A, B, and C are equivalent to cases b, d, and f, respectively, in Fig. 1.

The results of angle resolved light scattering measurements at 325 nm are shown in Fig. 3. It is very illustrative and intuitive that with increasing roughness, the intensity of the specularly reflected beam is decreased and at the same time the diffuse scattering is increased. This redistribution of power is consistent with the conservation of energy.

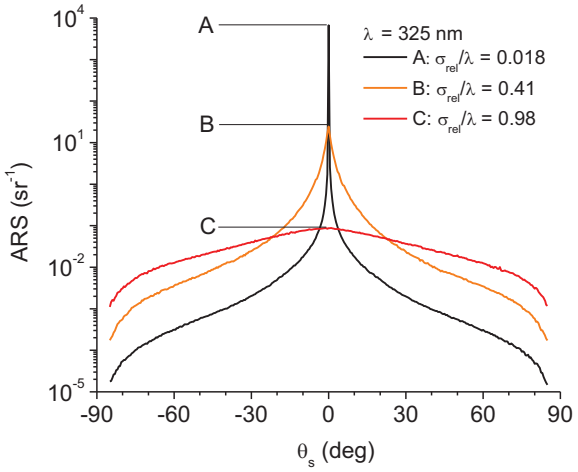

Fig. 3. Results of ARS measurements at 325 nm of steel surfaces with different surface structures represented as different roughness values. The heights of the specular peaks are indicated by horizontal bars.

The results of ARS measurements and predictions using the RR and the GHS theories for samples A, B, and C at three different wavelengths are shown in Fig. 4.

For the smoothest sample under investigation, sample A, the RR and the GHS results are virtually identical and in excellent agreement with the experiment data (Fig. 4(a)). Similar to the case shown in Fig. 1(b), the results demonstrate the accuracy of both the RR and the GHS for this optically smooth surface. In this regime, PSD and ARS are directly proportional and either of the functions can be determined by measuring the other. This is consistent with the fact that only the first diffracted orders of roughness components making up the stochastic surface contain significant power. The PSD can be easily calculated by analyzing the measured light scattering distribution using Eq. (6). This approach has been demonstrated to be very powerful for the characterization of optical surfaces [7,13,15,23].

#142704 - $15.00 USD Received 14 Feb 2011; revised 7 Apr 2011; accepted 1 May 2011; published 5 May 2011

Considering the shortest wavelength used and the roughness of the sample the results suggest that the smooth surface criterion can be formulated as: $\sigma_{rel} \cos \theta_i / \lambda \leq 0.02$. This is in reasonable agreement with the results of Sec. 5 and former statements [13,15]. Since $TS_b/R \leq (4\pi\sigma_{rel} \cos \theta_i / \lambda)^2$ [3,13], where R denotes the specular reflectance, an alternative criterion for the total scattering instead of the roughness allowed would be $TS_b/R \leq 0.07$. Based on the results of Sec. 5 we believe that the smooth surface approximation might still be valid in particular at large angles even if these conditions are violated to some extent. If a surface does not meet the smooth surface requirement at a short wavelength or small incident angles, a larger wavelength or incident angle may be used in order to determine the surface PSD from scatter measurements. However, measurements at short wavelengths might still be required to obtain information about high spatial frequency roughness components.

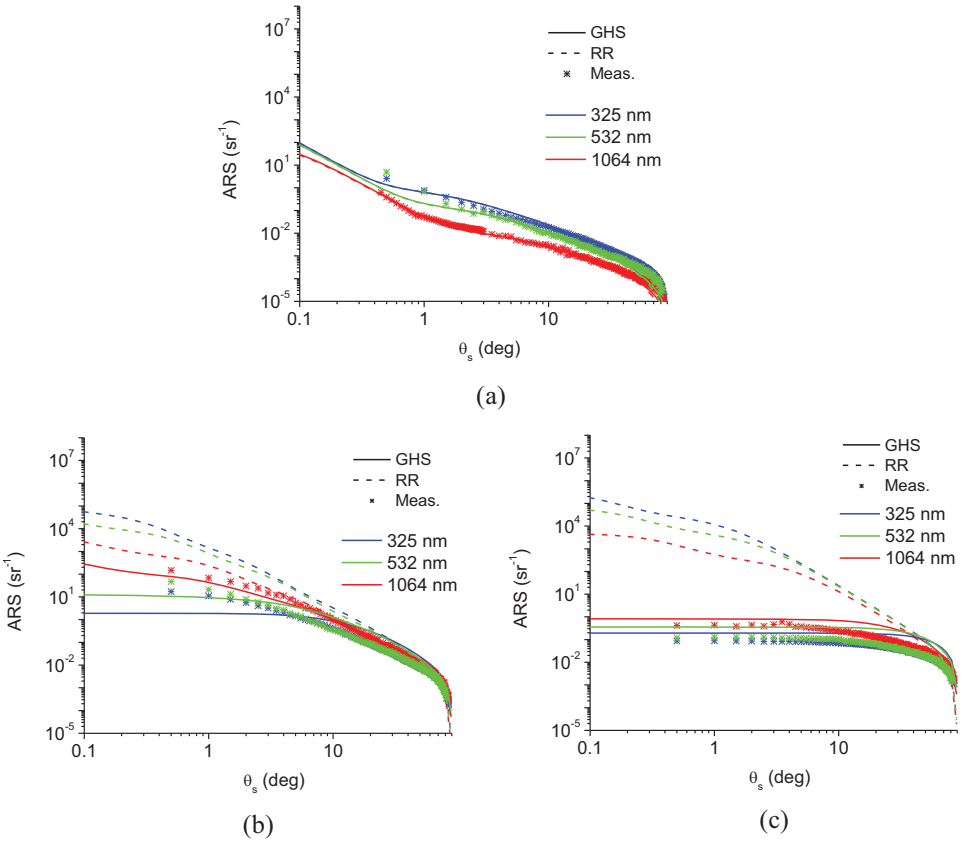

Fig. 4. ARS of surfaces with different roughness levels. Measurement results at 325 nm, 532 nm, and 1064 nm and modelling using the Rayleigh-Rice theory (RR) and the Generalized Harvey-Shack theory (GHS). (a) sample A, (b) sample B, and (c) sample C at 325 nm, 532 nm, and 1064 nm.

The results for sample B are shown in Fig. 4(b). With a roughness to wavelength ratio between 0.12 and 0.41 depending on the wavelength this sample represents a moderately rough surface corresponding to the grating results shown in Fig. 1(d). As already mentioned, the RR theory is not supposed to be valid in this case. The results clearly show that the ARS is tremendously overestimated in particular at smaller angles, whereas a remarkably good agreement can still be observed at large angles. The GHS results correctly describe the behavior of the scattering curve being damped at smaller angles compared to the linear relationship of the PSD and the ARS predicted by the RR theory. This is similar to the

#142704 - $15.00 USD Received 14 Feb 2011; revised 7 Apr 2011; accepted 1 May 2011; published 5 May 2011

observation for sinusoidal gratings that for increasing amplitude the first order diffraction efficiency is reduced in favor of higher orders. And the highest roughness amplitudes in the PSDs usually occur at smaller spatial frequencies corresponding to small scatter angles. Because of the mixing of higher diffracted orders of different roughness components at the same scatter angles solving the inverse scattering problem directly is not possible. Yet it might be possible to tackle this problem using the GHS theory and reverse engineering based on varying the input PSDs. It is interesting to note that in this regime the reflectance properties of the surface determine the ARS level in contrast to the dominating $1/\lambda^4$ wavelength relationship predicted by the RR theory.

Even though there is reasonable agreement between the experimental and GHS results, considerable discrepancies can be observed in particular at 325 nm. We believe this is more likely caused by the sample properties and uncertainties in the experimental data rather than by inaccuracies of the theoretical models. In general, the following facts have to be considered when comparing measured light scattering data and modeling results based on measured surface PSDs: (i) Both AFM and WLI measurement results are influenced by measurement uncertainties that are seldom given explicitly but can be assumed to be approximately 10-30%. In addition, for the scatter modeling, ABC model functions were fitted to the experimental data. This might both reduce fluctuation effects as well as lead to additional errors. (ii) The scattering measurements exhibit a relative uncertainty that has been determined to be about 10%. Surface speckle effects are suppressed by choosing a sufficiently large detector solid angle. (iii) If the roughness is not perfectly homogeneous, the PSDs determined from a roughness measurement at one position and the PSD relevant for the scattering measured at another position are not equal. (iv) If the roughness is not perfectly isotropic, the measured in-plane ARS corresponds to a one dimensional slice of the 3D surface PSD whereas the Master PSDs have been calculated by averaging over all directions.

Because the RR theory is not valid anymore over the entire angular range, it is not possible to obtain the PSD directly from ARS measurements at the given wavelengths for sample B. However, in this intermediate roughness regime, referred to as the specular regime in [15], there is still a pronounced specular peak that may be used to calculate the rms roughness. In addition, the inverse scattering problem may be solved by recursively applying the GHS theory.

Sample C is the roughest of the samples investigated. The ARS modeling and measurement results are shown in Fig. 4(c). Again, the GHS prediction is in reasonable agreement with the experimental results. The obvious deviations in the absolute value are again believed to be caused by the inhomogeneity of the sample, whereas the deviations at scatter angles >10° might be caused by an anisotropy of the surface roughness. The ARS curves of sample C illustrate that already for a roughness to wavelength ratio greater than 0.2 there will be no specular beam anymore. However, even in this diffuse regime the rms roughness may still be retrieved from analyzing the Total Scattering directly. Though, the limitations of this approach have to be investigated carefully. Recent investigations suggested modifications of the established models that shall not be discussed further in the present paper.

Even though the uncertainties involved in using real experimental data for both the scatter measurements and the input for the scatter modeling the results discussed above demonstrate that the GHS theory can be used to predict the scattering properties for different regimes of surface roughness. The good agreement of the RR theory in particular at very large angles even if the smooth surface criterion is clearly violated suggests that an obliquity correction factor might be applied to the GHS theory to further increase the accuracy at all scatter angles.

7. Summary and conclusions

Different approaches were used to predict the angle resolved scattering of metal surfaces in roughness regimes from optically smooth to moderately and very rough.

#142704 - $15.00 USD Received 14 Feb 2011; revised 7 Apr 2011; accepted 1 May 2011; published 5 May 2011

It has been confirmed that the Rayleigh-Rice (RR) vector perturbation theory yields highly accurate results as long as the smooth surface criterion $(4\pi\sigma_{rel} \cos \theta_i / \lambda)^2 << 1$ is met. As a quantitative criterion, the surface can be considered optically smooth if: $\sigma_{rel} \cos \theta_i / \lambda \leq 0.02$ or, equivalently, if $TS_b/R \leq 0.07$. In this regime, only the first diffracted orders of roughness components contain significant power. PSD and ARS are directly proportional and either of the functions can be determined by measuring the other.

In the smooth surface regime the predictions of the Generalized Harvey-Shack (GHS) scattering theory are almost identical to the RR results except for a slightly different obliquity factor. Investigations of sinusoidal phase gratings demonstrated that the RR result is in perfect agreement with rigorous modeling using Rigorous Coupled Wave analysis. This suggests that an obliquity correction factor might be applied to the GHS result.

For moderately rough surfaces the RR theory starts to overestimate the ARS in particular at small scattering angles. This corresponds to the beginning of specular power being redistributed not only to first but also to higher diffracted orders. Nevertheless, the GHS theory accurately takes into account these higher order effects.

Even for very rough surfaces the GHS theory yields results that are in reasonable agreement with experimental data. Because of the mixing of higher diffracted orders of different roughness components, solving the inverse scattering problem directly is not possible. However, PSD information might be retrieved using the GHS theory and reverse engineering based on varying the input PSDs. Since the RR theory still provides remarkable accurate results at very large scattering angles even if the smooth surface criterion is clearly violated, it might be used to provide initial results for the reverse engineering procedure.

In summary, it has been demonstrated that the GHS theory allows us to predict the angle resolved scattering of arbitrary stochastically rough surfaces without restrictions on the surface roughness and the surface autocorrelation function.

However, the accuracy of the prediction also depends on the quality of the surface metrology data used as input. This comprises not just the uncertainty of the measurements but also the homogeneity, isotropy, and defectivity of the surface. In some cases, it might therefore be desirable to perform direct light scattering measurements instead of or in addition to scatter modeling. Furthermore, the investigations presented in this paper were confined to single surfaces. The scattering of optical and non-optical coatings usually involves a substantially increased degree of complexity such that direct measurements at the wavelength of application are often the easiest and most reliable way to characterize their light scattering properties even though simplified modeling approaches for multilayer coatings exist [28].

Acknowledgments

The contributions of Tobias Herffurth, Matthias Hauptvogel, Alexander von Finck, Ralf Steinkopf, Gilbert Leibeling (all IOF), and Stephanie Fischer (Inst. Materials Science and Technology, FSU Jena) to sample preparation and measurements are gratefully acknowledged. We also thank Narak Choi (CREOL) and Thomas Germer (NIST, Gaithersburg) for providing their algorithms for the RCWA calculations. Financial support of this work was provided by the German Federal Ministry for Education and Science (BMBF) application center amos, project MORIN; and the BMBF program “Energieeffizienz in der Produktion,” project SmartSurf.

#142704 - $15.00 USD Received 14 Feb 2011; revised 7 Apr 2011; accepted 1 May 2011; published 5 May 2011